Supporting Information

Synthesis of a twisted aza-nanographene featuring a diquinoxaline-fused pyrene

Zhiyu Zhang,[1] Zhenxun Xu,[1] Aihui Zhang,[1] Fenghua Bai,[1]*
Yoshifumi Hashikawa,[2]* and Chaolumen[1]*

[1]*College of Chemistry and Chemical Engineering, Inner Mongolia University, Hohhot, 010021, China*
[2]*Institute for Chemical Research, Kyoto University, Uji, Kyoto 611-0011, Japan*

E-mail: f.h.bai@imu.edu.cn; hashi@scl.kyoto-u.ac.jp; chaolumen@imu.edu.cn

Contents

1. General

The ^{1}H and ^{13}C NMR measurements were carried out with a Bruker AVANCE NEO 600 MHz instrument. The NMR chemical shifts are reported in ppm with reference to residual protons and carbons of $CDCl_3$ (δ 7.26 ppm in ^{1}H NMR, δ 77.16 ppm in ^{13}C NMR). UV-vis absorption spectra were measured with a Shimadzu UV-3600i Plus spectrometer. The fluorescence spectra were measured with a Hitachi F-4700 Fluorescence spectrometer. The absolute fluorescence quantum yields were measured using a Hamamatsu Photonics Quantaurus QY C11347-11 with calibrated integrating sphere system. Matrix-Assisted Laser Desorption/ Ionization Time of Flight (MALDI-TOF) mass spectra were measured on a Shimadzu AXIMA Performance spectrometer. FT-IR spectra were taken with a Bruker Vertex 70 FTIR spectrometer. Cyclic voltammetry (CV) was performed on a CHI 760E electrochemical analyzer. The CV cell consists of a glassy carbon electrode, a Pt wire counter electrode, and an Ag/AgCl reference electrode. The measurements were carried out under a nitrogen atmosphere using 1 mM sample solutions in CH_2Cl_2 with 0.1 M tetrabutylammonium hexafluorophosphate (n-$Bu_4N^+PF_6^-$) as a supporting electrolyte. The redox potentials were calibrated with ferrocene as an internal standard.

Silica gel used for column chromatography was purchased from NUO TAI with a grain size of 0.063–0.200 mm. Preparative gel permeation chromatography (GPC) was performed with a Labo ACE 5060 P2.

CH_2Cl_2 (dehydrated), CH_3CN (dehydrated), and $RuCl_3$ were purchased from Beijing InnoChem Science & Technology Co. DDQ (2,3-dichloro-5,6-dicyano-*p*-benzoquinone), TfOH (Tf: triflate), AcOH (Ac: acetyl), *o*-phenylenediamine, and $NaIO_4$ were purchased from Shanghai Macklin Biochemical Technology Co., Ltd. *n*-Hexane and CH_2Cl_2 were purchased from Shanghai Titan Technology Co., Ltd. $CHCl_3$, NaCl, $NaHCO_3$, and Na_2SO_4 were purchased from Tianjin Wind Boat Chemical Reagent Technology Co., Ltd. Unless otherwise noted, all commercial reagents and solvents are used as received and no further purification was performed.

3,5',3''-tri(*tert*-butyl)-2'-iodo-1,1':3',1''-terphenyl (**1**)[1] were prepared according to literature procedures. All reactions were carried out under a nitrogen atmosphere.

2. Computational Methods

All calculations were performed using the Gaussian 09 program. All structures at the stationery states were optimized at the B3LYP-D3/6-31G(d) level of theory without any symmetry assumptions and confirmed by frequency analysis at the same level of theory. The NICS (nucleus-independent chemical shift) calculations were performed at the HF/6-31+G(d,p) level of theory using structures optimized at the aforementioned level. ACID (anisotropy of current-induced density) plots were generated at the B3LYP-D3/6-31G(d) level of theory using structures optimized at the aforementioned level. TD-DFT calculations were conducted at the TD-CAM-B3LYP-D3/6-31G(d) level of theory using the structure optimized at the aforementioned level.

3.Synthesis

3.1. Synthesis of 2

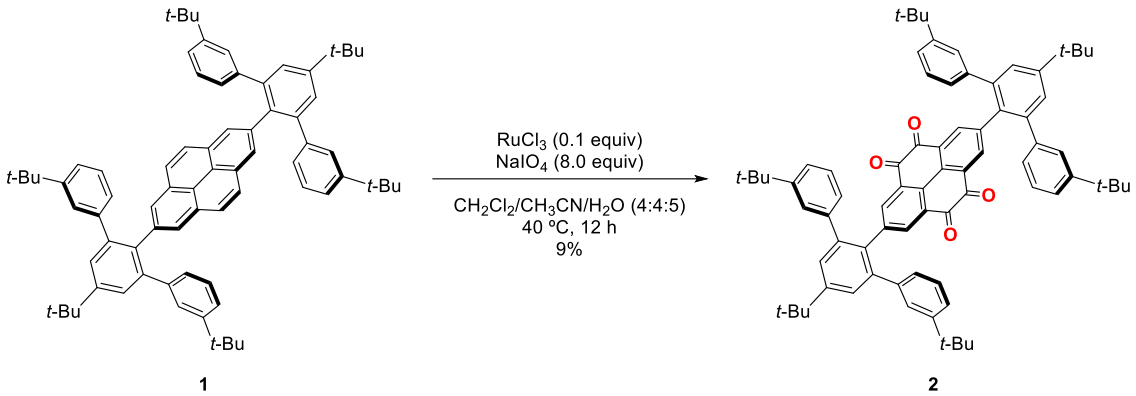

Powdery **1** (2.2 g, 2.2 mmol), $RuCl_3$ (46 mg, 0.22 mmol, 0.1 equiv), and $NaIO_4$ (3.8 g, 18 mmol, 8.0 equiv) were added into a 500 mL two-neck flask and degassed through three vacuum–N_2 cycles. CH_2Cl_2 (80 mL), CH_3CN (80 mL), and H_2O (100 mL) were added and stirred at 40 °C for 12 h (oil bath). The mixture was poured into distilled water and extracted with CH_2Cl_2 (50 mL × 3). The combined organic layer was washed with brine, dried over Na_2SO_4, filtrated, and evaporated. The resultant mixture was then purified by column chromatography using silica gel (CH_2Cl_2/*n*-hexane (1:4)) to give **2** (210 mg, 0.198 mmol, 9%) as an orange powder.

During the oxidation, nearly half of **1** was recovered and a pyrene-4,5-dione derivative was obtained as a major product in 15% yield. Even after extending the reaction time to four days, the yield of **2** remained unchanged.

2: ^{1}H NMR (600 MHz, $CDCl_3$) δ 7.81 (s, 4H), 7.50 (s, 4H), 7.17–7.12 (m, 8H), 7.08 (s, 4H), 6.96 (d, J = 7.0 Hz, 4H), 1.43 (s, 18H), 1.11 (s, 36H); ^{13}C NMR (151 MHz, $CDCl_3$) δ 177.55, 151.97, 150.89, 144.15, 142.13, 140.82, 139.64, 133.00, 131.40, 129.57, 128.08, 127.88, 127.13, 126.81, 123.80, 35.08, 34.67, 31.50, 31.33 (The sum of carbon signals must be 19 in theory. Observed 19). HRMS (MALDI-TOF) *m/z*: $[M]^{\bullet-}$ Calcd. for $C_{76}H_{78}O_4$ (**2**) 1054.5906; Found 1054.5901.

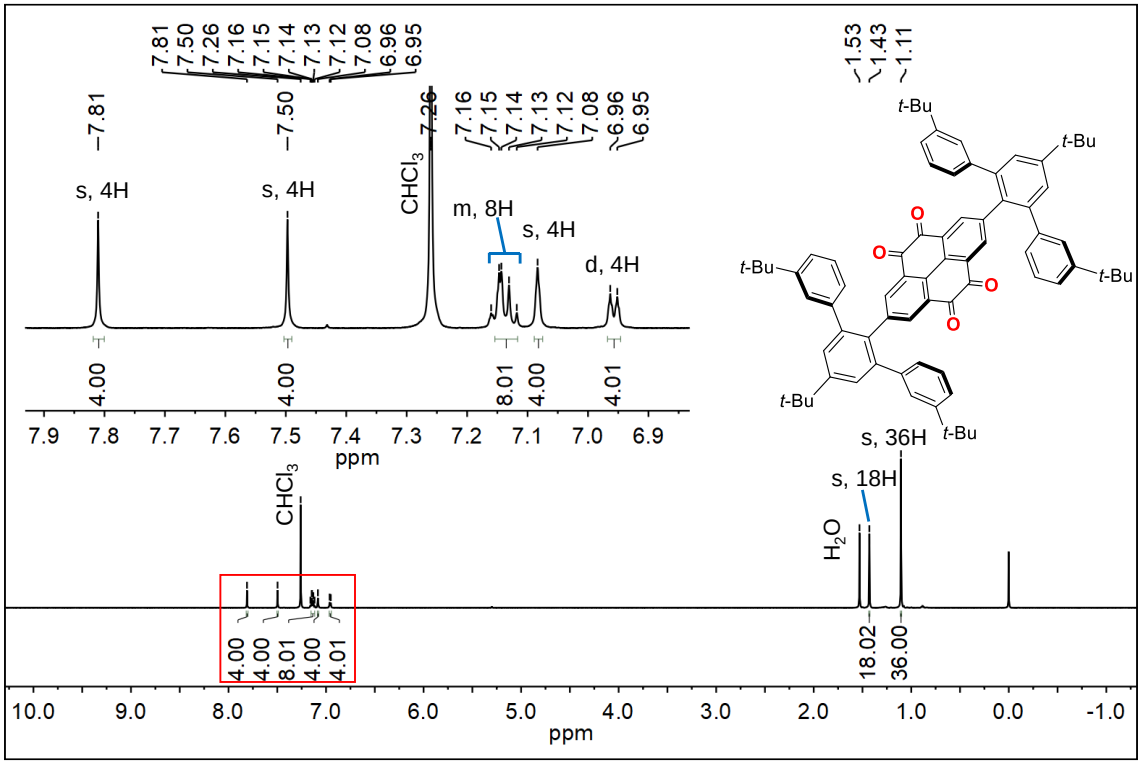

Figure S1. ^{1}H NMR spectra (600 MHz, $CDCl_3$) of **2**.

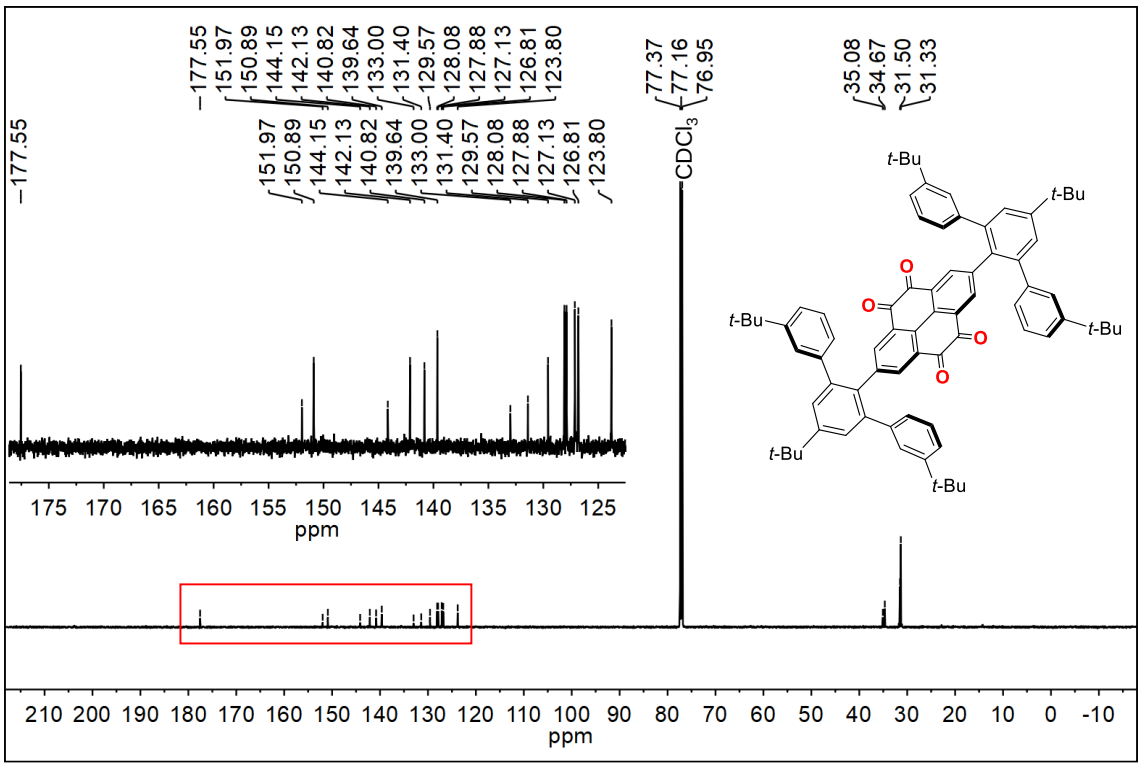

Figure S2. ^{13}C NMR spectra (151 MHz, $CDCl_3$) of **2**.

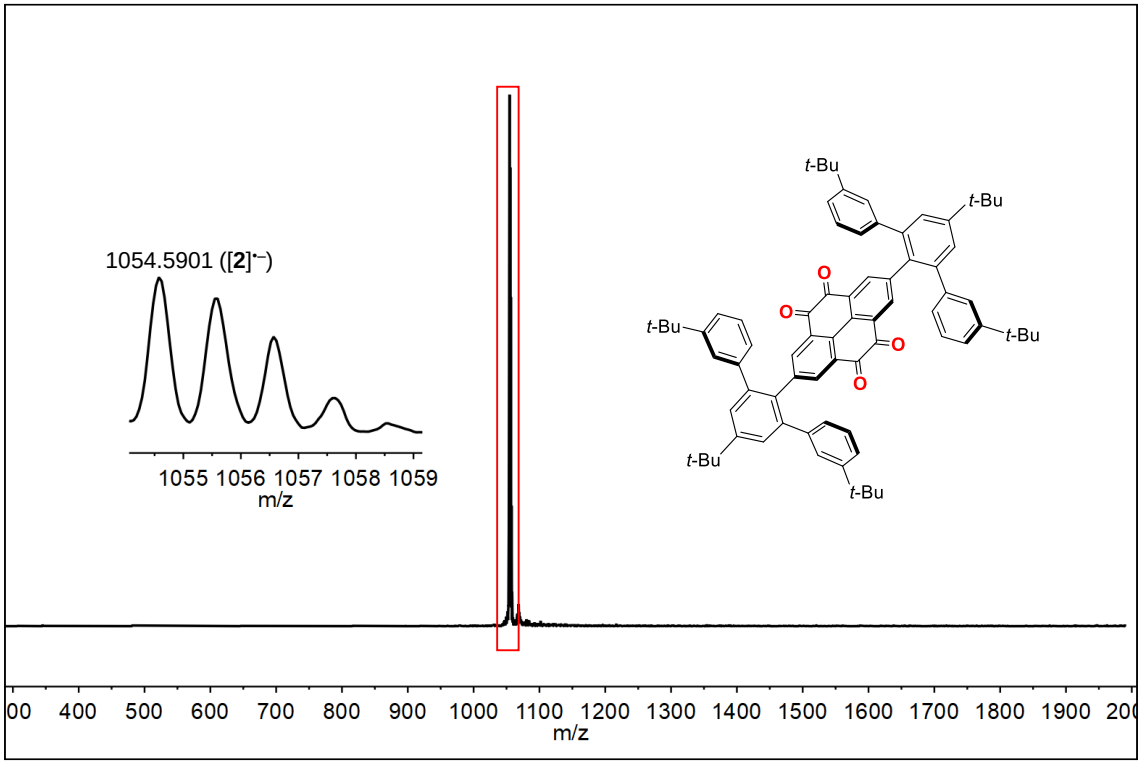

Figure S3. MALDI-TOF mass spectra (negative ion mode) of **2**.

3.2. Synthesis of 3

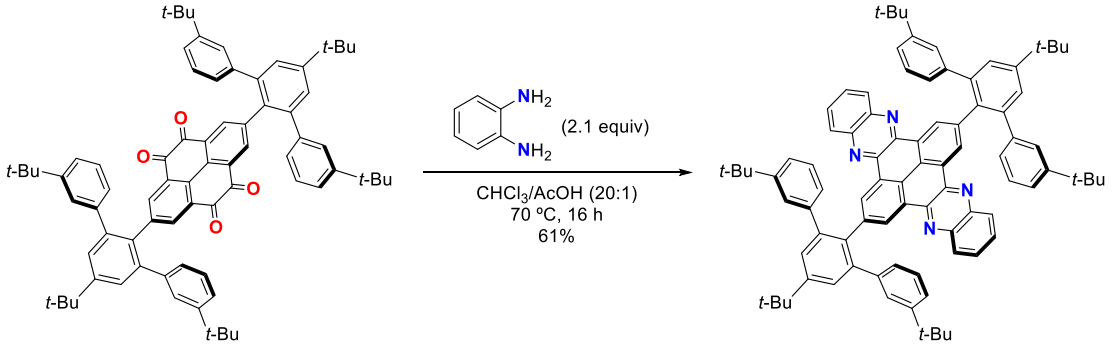

Powdery **2** (200 mg, 0.190 mmol) and *o*-phenylenediamine (43 mg, 0.40 mmol, 2.1 equiv) were added into a Schlenk tube and degassed through three vacuum–N_2 cycles. $CHCl_3$ (20 mL) and then AcOH (1 mL) were added. The reaction mixture was heated at 70 °C for 20 h (oil bath). After cooling down to room temperature, the mixture was carefully poured into saturated aqueous $NaHCO_3$ solution (ca. 10 mL) and extracted with CH_2Cl_2 (20 mL × 3). The combined organic layer was washed with brine, dried over Na_2SO_4, filtrated, and evaporated. The resultant mixture was then purified by column chromatography using silica gel (CH_2Cl_2/*n*-hexane (1:3)) to give **3** (139 mg, 0.120 mmol, 61%) as a yellow powder.

3: ^{1}H NMR (600 MHz, $CDCl_3$) δ 9.21 (s, 4H), 8.13 (dd, J = 3.4, 6.4 Hz, 4H), 7.78 (dd, J = 3.4, 6.4 Hz, 4H), 7.63 (s, 4H), 7.37 (s, 4H), 7.06 (d, J = 7.8 Hz, 4H), 6.92 (t, J = 7.8 Hz, 4H), 6.96 (d, J = 7.8 Hz, 4H), 1.52 (s, 18H), 0.86 (s, 36H); ^{13}C NMR (151 MHz, $CDCl_3$) δ 173.56, 150.65, 150.33, 142.80, 142.58, 142.36, 141.92, 136.73, 131.09, 129.61, 129.56, 128.79, 128.12, 127.39, 127.32, 126.63, 122.99, 35.07, 34.45, 31.71, 31.14 (The sum of carbon signals must be 22 in theory. Observed 21. One sp^2 signal is overlapped in aromatic region.); HRMS (MALDI-TOF) *m/z*: $[M]^{\bullet+}$ Calcd. for $C_{88}H_{86}N_4$ (**3**) 1198.6846; Found 1198.6853.

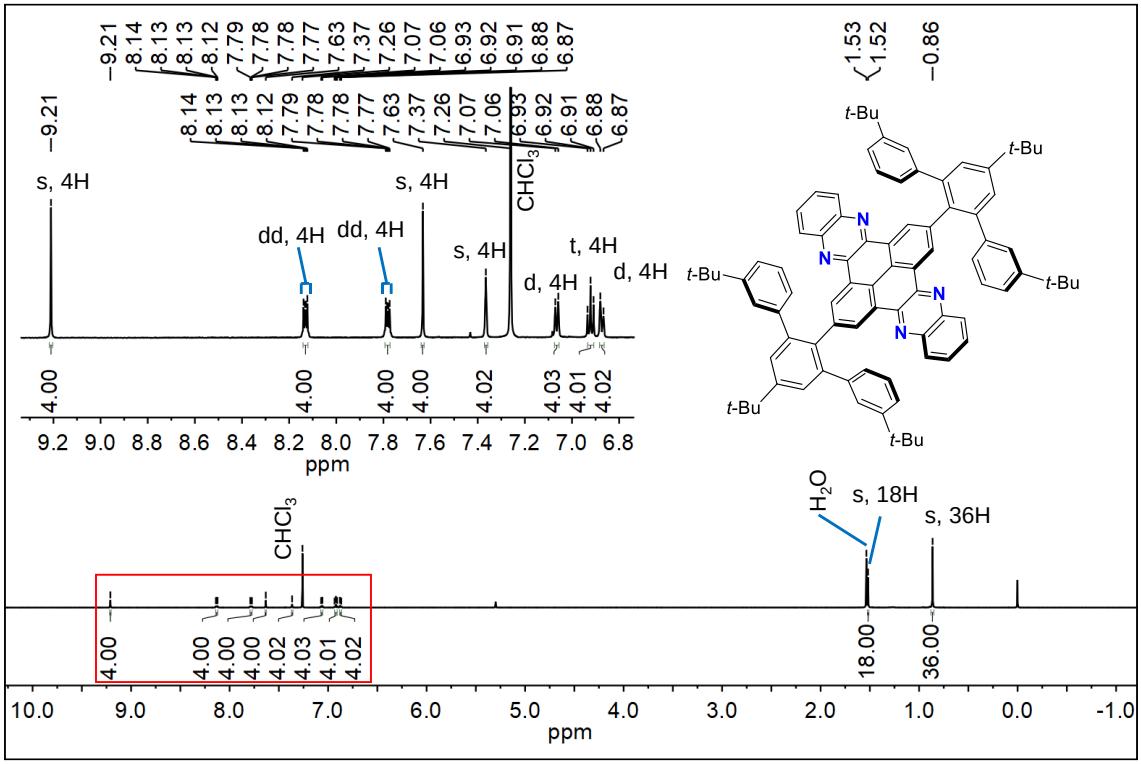

Figure S4. ^{1}H NMR spectra (600 MHz, $CDCl_3$) of **3**.

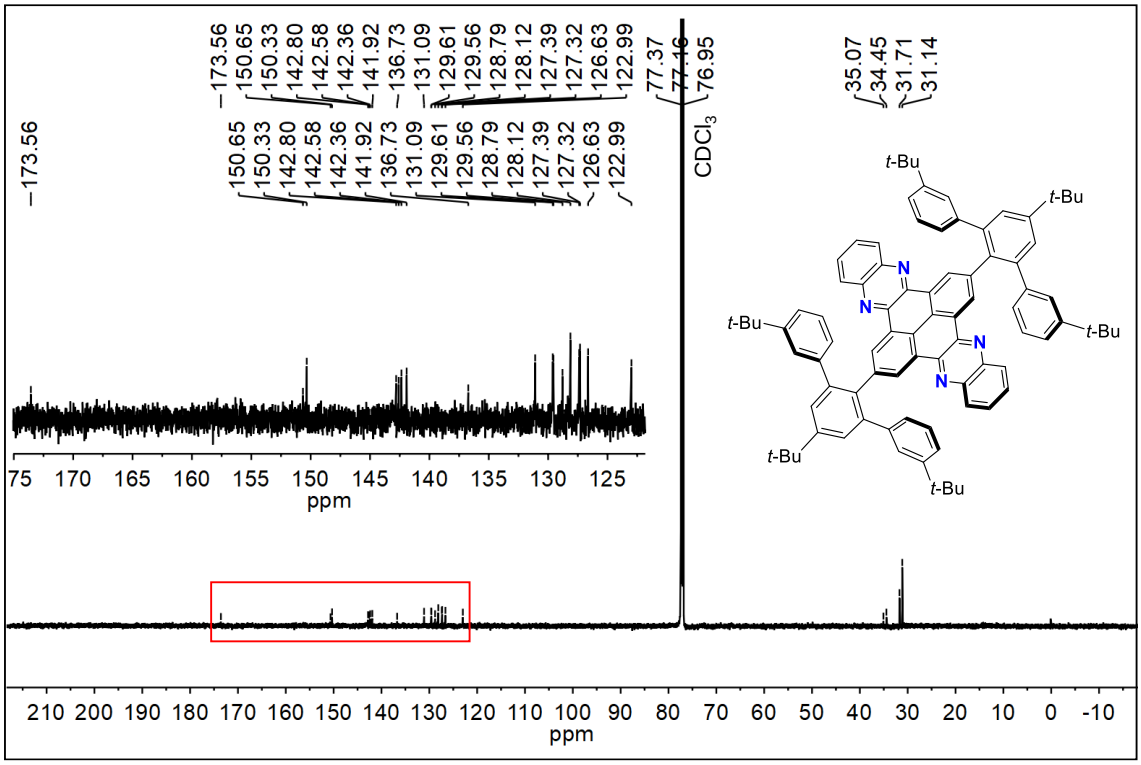

Figure S5. ^{13}C NMR spectra (151 MHz, $CDCl_3$) of **3**.

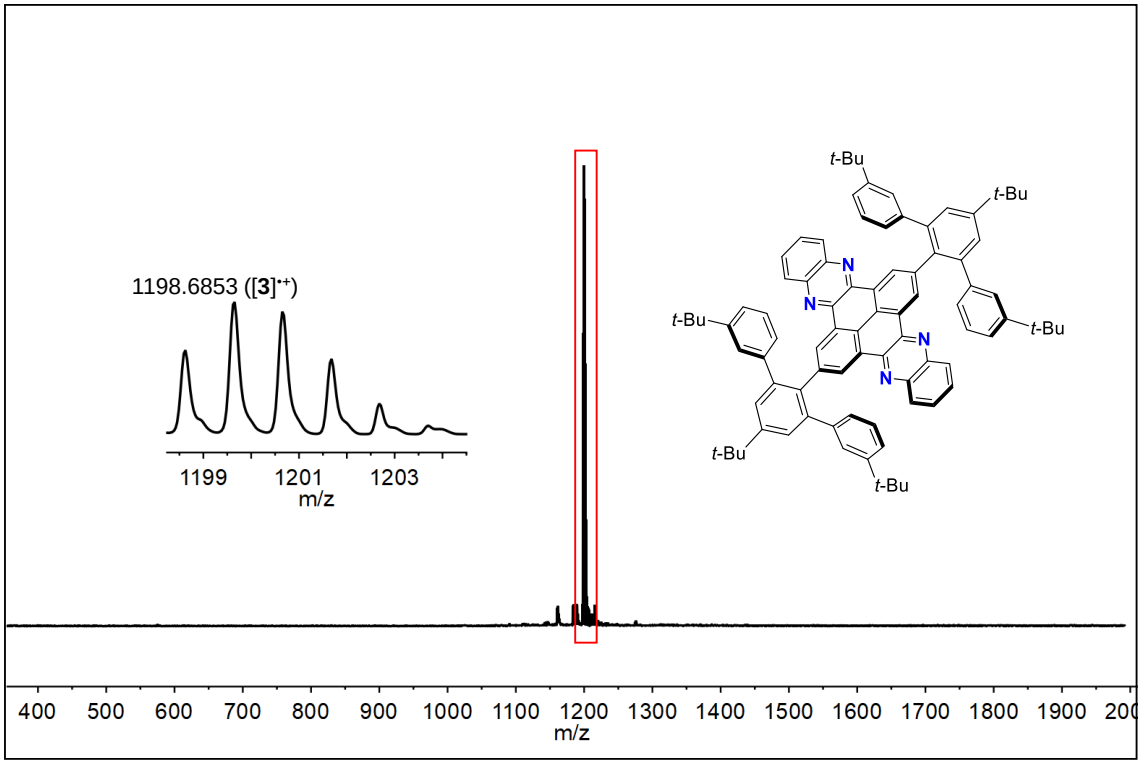

Figure S6. MALDI-TOF mass spectra (positive ion mode) of **3**.

3.3. Synthesis of 4

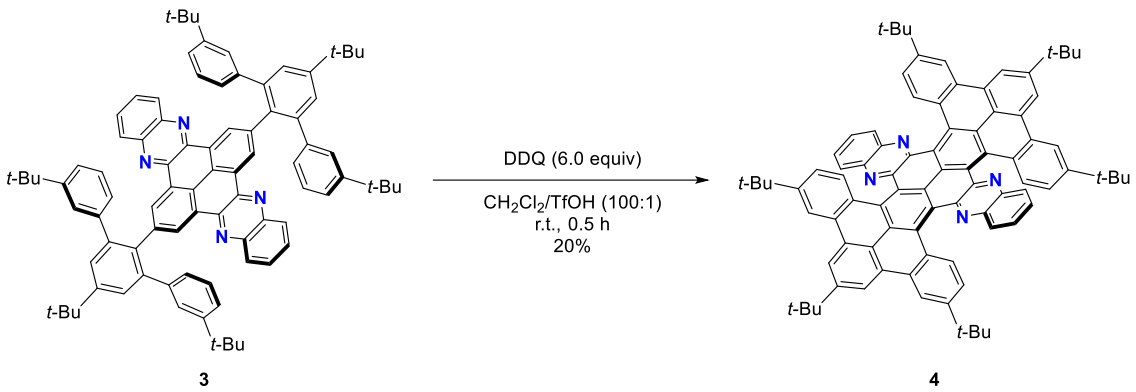

Powdery **3** (30 mg, 0.025 mmol) and DDQ (34 mg, 0.15 mmol, 6.0 equiv) were added into a 50 mL two-neck flask and degassed through three vacuum–N_2 cycles. Dry CH_2Cl_2 (20 mL) was added. After the reaction mixture was stirred at room temperature for 5 min, TfOH (0.2 mL) was added and stirred for additional 0.5 h. The mixture was quenched by an excessive amount of hydrazine (ca. 0.6 mL) and extracted with CH_2Cl_2 (20 mL × 3). The combined organic layer was washed with brine, dried over Na_2SO_4, filtrated, and evaporated. The reaction mixture was then purified by column chromatography using silica gel (CH_2Cl_2/*n*-hexane (1:1)) to give **4** (6.0 mg, 5.0 μmol, 20%) as a red powder.

The optimization of the reaction conditions was performed by changing the amount of oxidant, the addition ratio of acid, and reaction time. The reaction with DDQ of 5 equiv. or less gave fully-cyclized **4** in an yield lower than 10% while bis- and tris-cyclized products were generated in ca. 50%. When DDQ was increased to 6 equiv., the yield of **4** increased to 20% while partially cyclized products was obtained in ca. 40%. When 8 equiv. of DDQ was employed, only junk materials were generated without isolable amount of cyclized products. Changing the ratio of the solvent system from CH_2Cl_2/TfOH (100:1) to (10:1) did not improve the yield of **4**. Higher temperature and longer reaction time didn't show positive effects for improving the yield of **4**.

4: ^{1}H NMR (600 MHz, $CDCl_3$) δ 9.23 (s, 4H), 8.94 (s, 4H), 8.69 (d, J = 8.7 Hz, 4H), 7.73 (dd, J = 3.3, 6.5 Hz, 4H), 7.62 (dd, J = 3.3, 6.5 Hz, 4H), 7.49 (d, J = 8.7 Hz, 4H), 1.81 (s,

18H), 1.60 (s, 36H); ^{13}C NMR (151 MHz, $CDCl_3$) δ 151.17, 149.56, 144.28, 141.42, 137.38, 132.81, 132.27, 131.28, 130.72, 129.60, 129.16, 128.65, 126.59, 126.34, 123.56, 120.11, 119.32, 118.79, 35.88, 35.47, 32.15, 31.51 (The sum of carbon signals must be 22 in theory. Observed 22). HRMS (MALDI-TOF) *m/z*: $[M]^{\bullet+}$ Calcd. for $C_{88}H_{78}N_4$ (**4**) 1190.6220; Found 1190.6222.

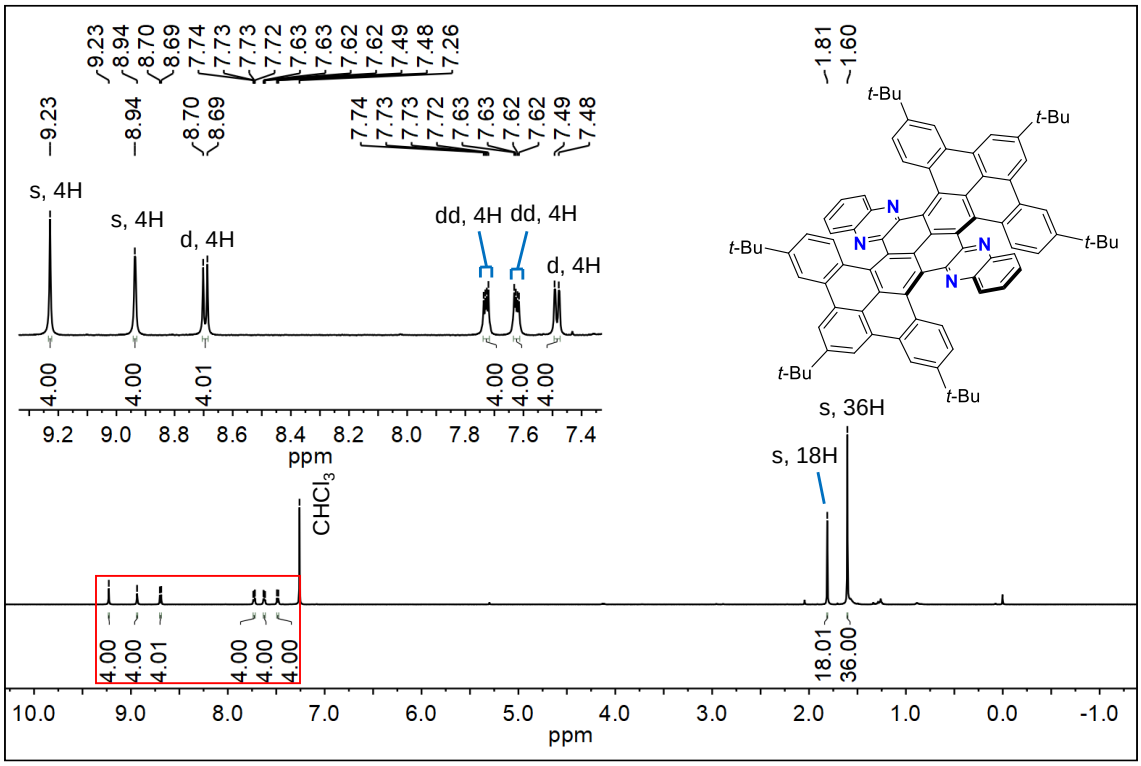

Figure S7. ^{1}H NMR spectra (600 MHz, $CDCl_3$) of **4**.

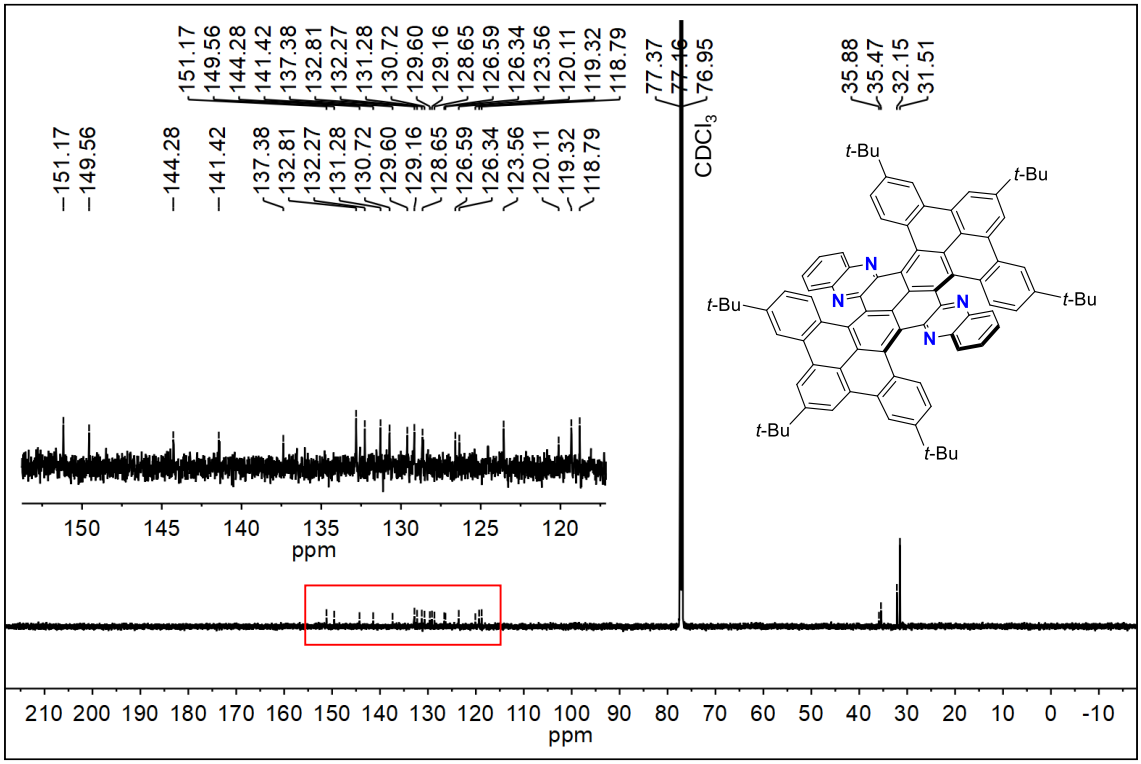

Figure S8. ^{13}C NMR spectra (151 MHz, $CDCl_3$) of **4**.

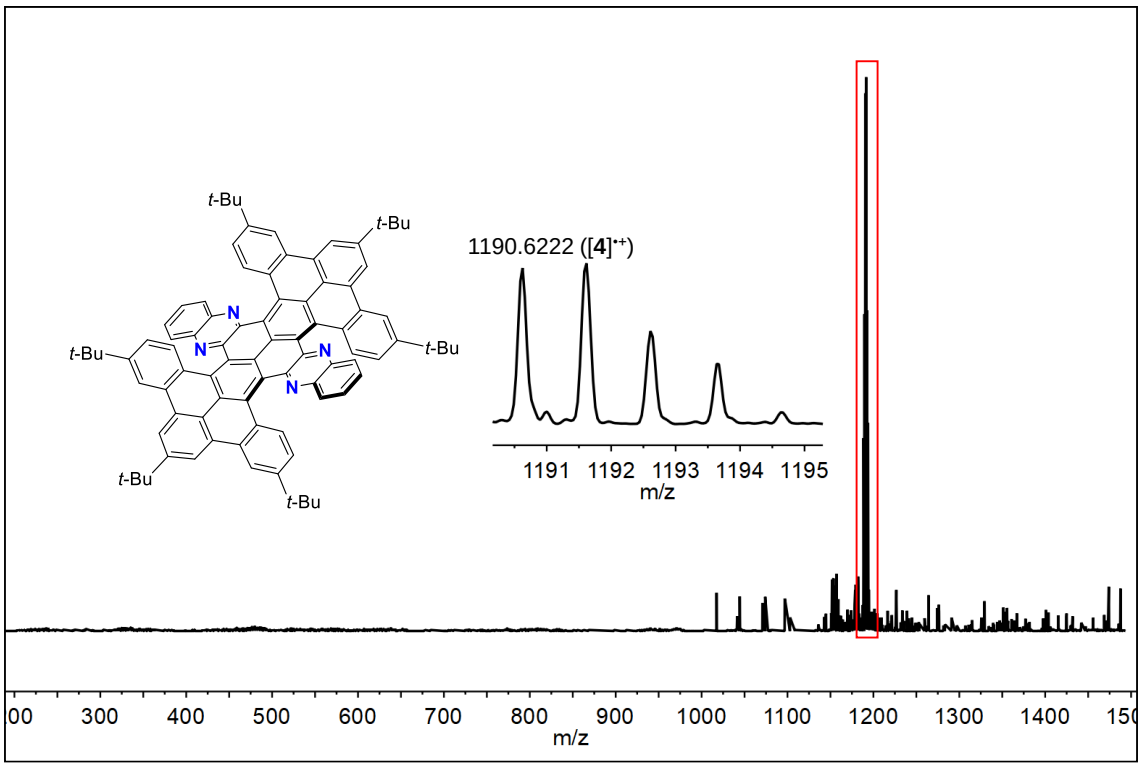

Figure S9. MALDI-TOF mass spectra (positive ion mode) of **4**.

4. Single-Crystal X-Ray Structure

Single crystals of **4** were grown from a CH_2Cl_2/*n*-hexane solution. Intensity data were collected at 100(2) K on a ROD, Synergy Custom system, HyPix-Arc 150 with Cu Kα radiation (λ = 1.54184 Å) and graphite monochromater. A total of 33573 reflections were measured at the maximum 2θ angle of 145.49°, of which 8178 were independent reflections (R_{int} = 0.0290). The structure was solved by direct methods (SHELXT-2018/2[2]) and refined by the full-matrix least-squares on F^2 (SHELXL-2018/3[2]). All non-hydrogen atoms were refined anisotropically. The crystal data are as follows: $C_{50.20}H_{52.96}Cl_{3.06}N_2$, FW = 792.68, crystal size 0.15 × 0.11 × 0.09 mm^3, Triclinic, *P*-1, a = 9.4575(3) Å, b = 13.1091(4) Å, c = 17.8161(6) Å, α = 83.827(2)°, β = 84.966(2)°, γ = 82.326(2)°, V = 2184.22(12) Å^3, Z = 2, D_c = 1.205 g cm^{-3}. The refinement converged to R_1 = 0.0642, wR_2 = 0.1772 (I > 2σ(I)), GOF = 1.041. The data was deposited at the Cambridge Crystallographic Data Centre (CCDC 2438323).

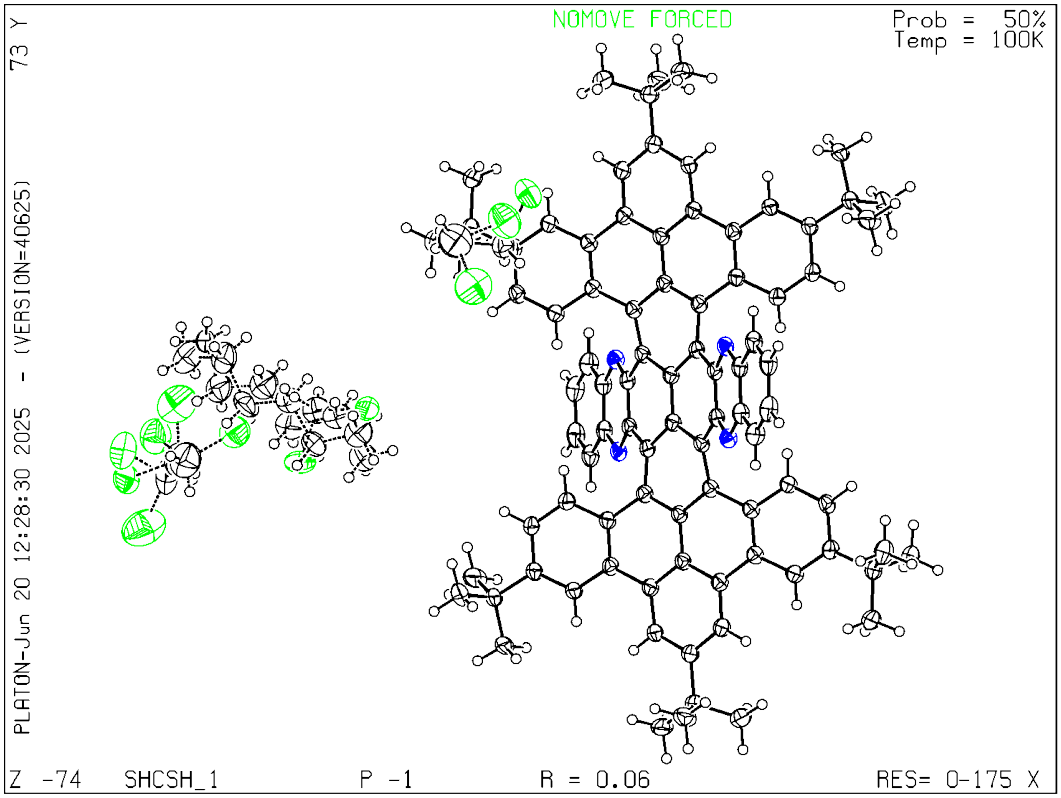

Figure S10. Crystal structure of **4** (50% probability for thermal ellipsoids).

5. Theoretical Calculations

5.1. TD-DFT Calculations

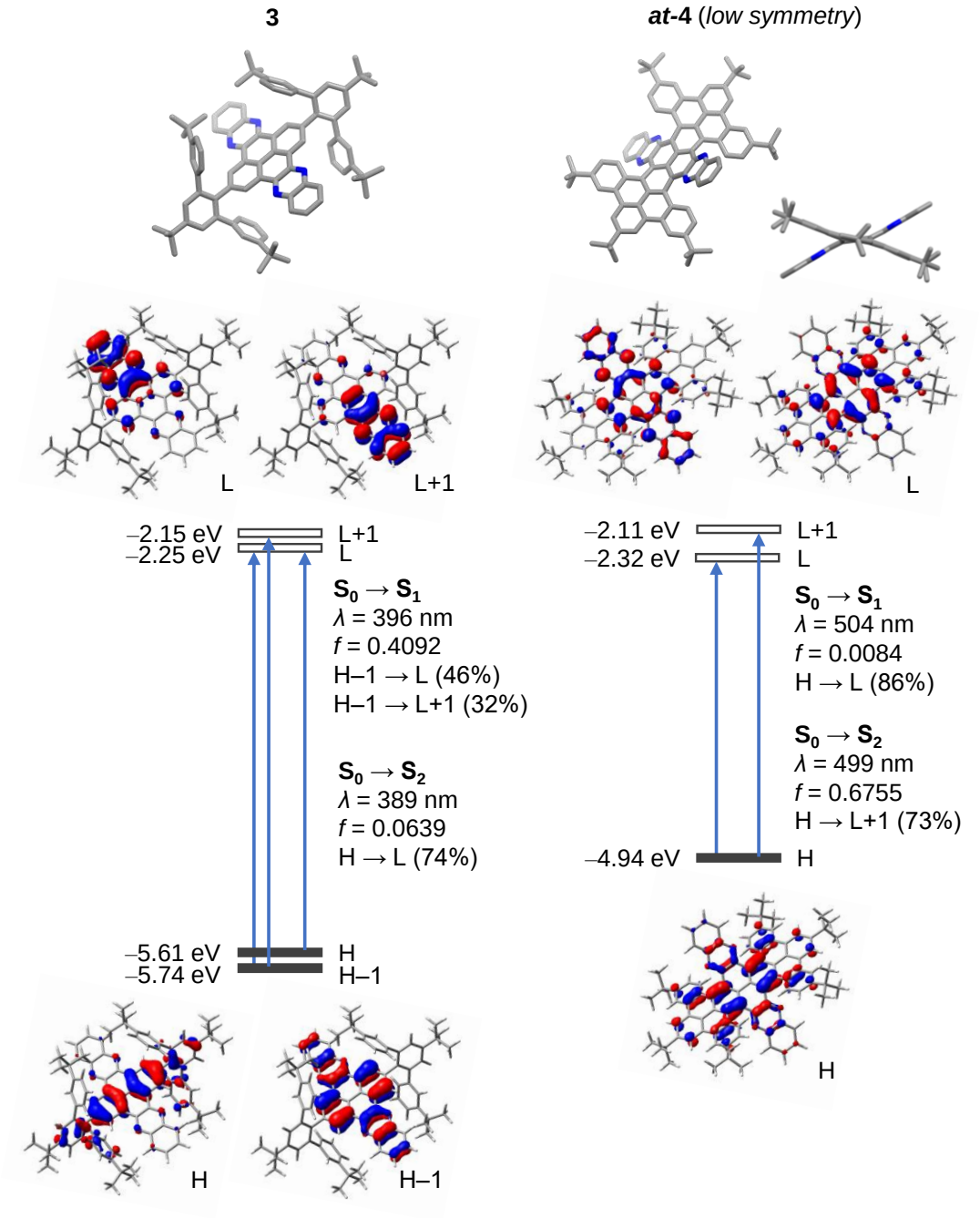

Figure S11. Relative energies (ΔG (kcal/mol) at 298 K) and pictorial representation of the frontier orbitals with selected optical transitions (TD-CAM-B3LYP-D3/6-31G(d)// B3LYP-D3/6-31G(d)) for **3** and ***at*-4** (*low symmetry*) at ground state. The transition energies were calibrated with a factor of 0.88.

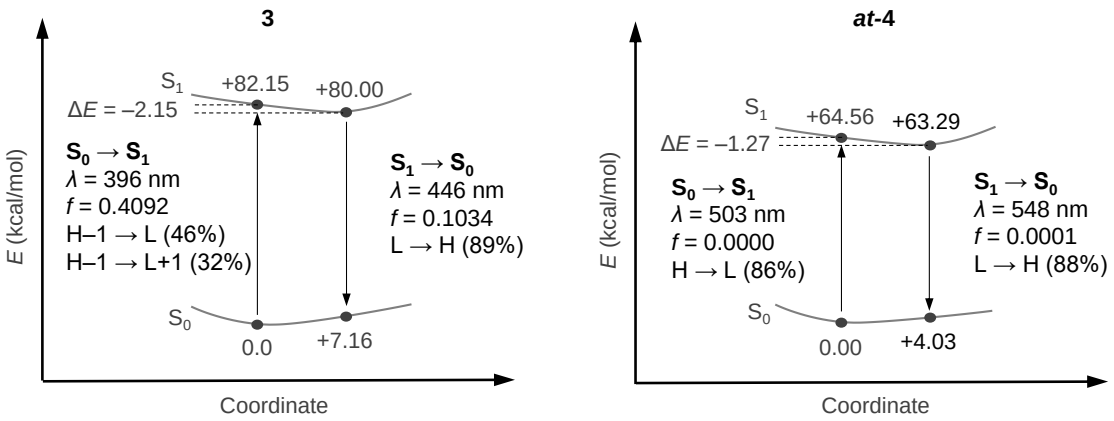

Figure S12. Relative energies (Δ*E* (kcal/mol) at 298 K) and optical transitions (TD-CAM-B3LYP-D3/6-31G(d)//B3LYP-D3/6-31G(d)) for **3** and ***at*-4** at ground state and excited state. The transition energies were calibrated with a factor of 0.88.

5.2. Possible Conformations of 4

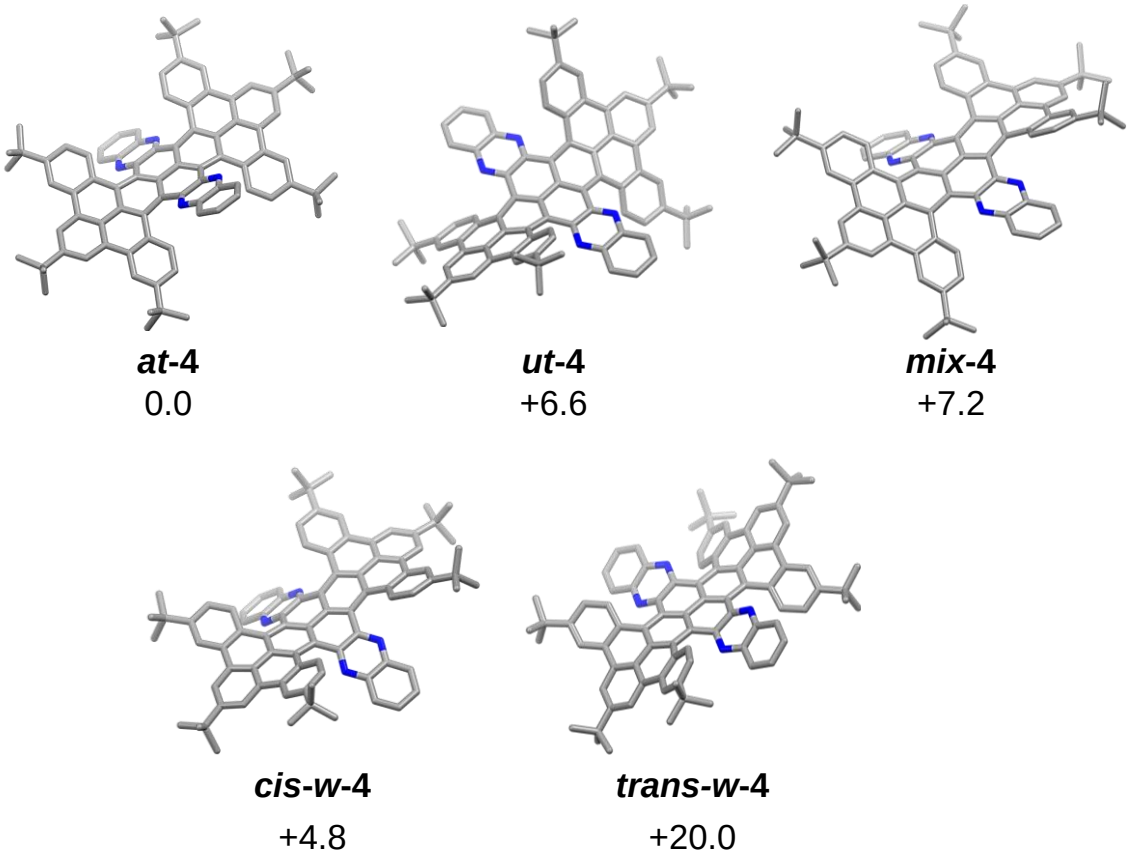

Figure S13. Relative energies (ΔG (kcal/mol) at 298 K)（B3LYP-D3/6-31G(d)) for ***at*-4**, ***ut*-4**, ***mix*-4**, ***cis*-*w*-4**, and ***trans*-*w*-4**.

The supplementary molecular coordinates for theoretical calculations were provided separately. The following tables represent the lists of coordinates.

Table S1. (**3** (ground state), B3LYP-D3/6-31G(d), total electronic energy –3624.5988057 Hartree)

Table S2. (**3** (excited state), B3LYP-D3/6-31G(d), total electronic energy –3624.5903562 Hartree)

Table S3. (***at*-4** (ground state), B3LYP-D3/6-31G(d), total electronic energy –3619.7997881 Hartree)

Table S4. (***at*-4** (excited state), B3LYP-D3/6-31G(d), total electronic energy –3619.7962279 Hartree)

Table S5. (***at*-4** (ground state, low symmetry), B3LYP-D3/6-31G(d), total electronic energy –3619.8011527 Hartree)

Table S6. (***ut*-4**, B3LYP-D3/6-31G(d), total electronic energy –3619.7931881 Hartree)

Table S7. (***cis*-*w*-4**, B3LYP-D3/6-31G(d), total electronic energy –3619.7945699 Hartree)

Table S8. (***trans*-*w*-4**, B3LYP-D3/6-31G(d), total electronic energy –3619.7714737 Hartree)

Table S9. (***mix*-4**, B3LYP-D3/6-31G(d), total electronic energy –3619.7896961 Hartree)

Table S10. (**diquinoxaline-fused pyrene**, B3LYP-D3/6-31G(d), total electronic energy –1294.5574126 Hartree)

6. FT-IR Spectra

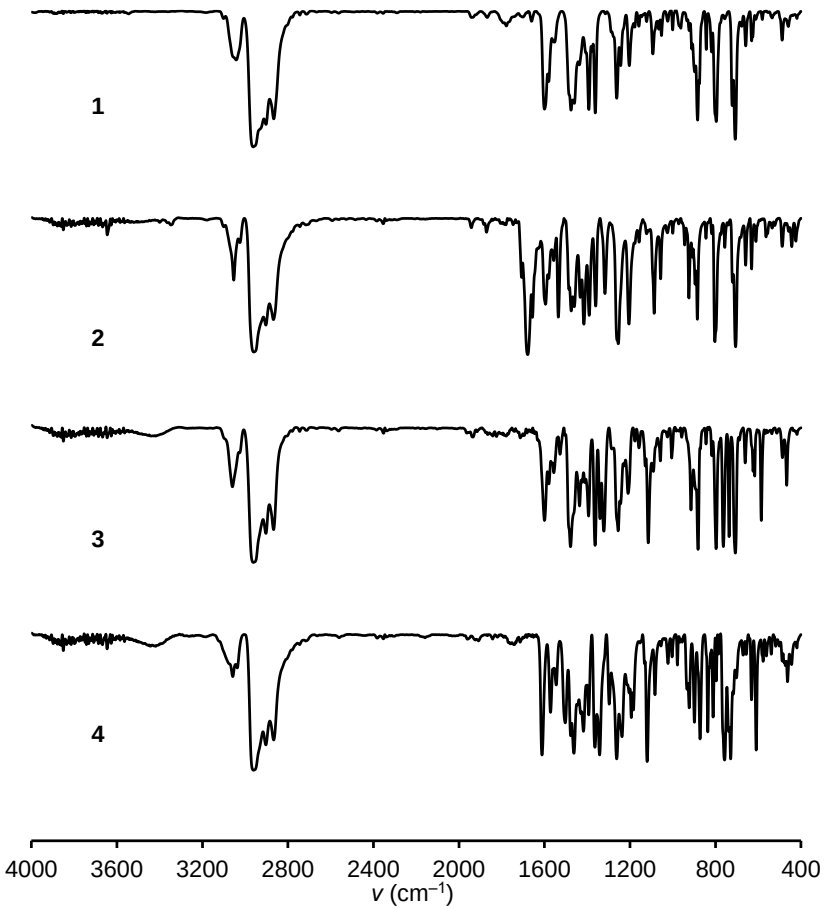

Figure S14. FT-IR spectra (KBr) of **1**, **2**, **3**, and **4**.

7. XRD Spectrum from CIF

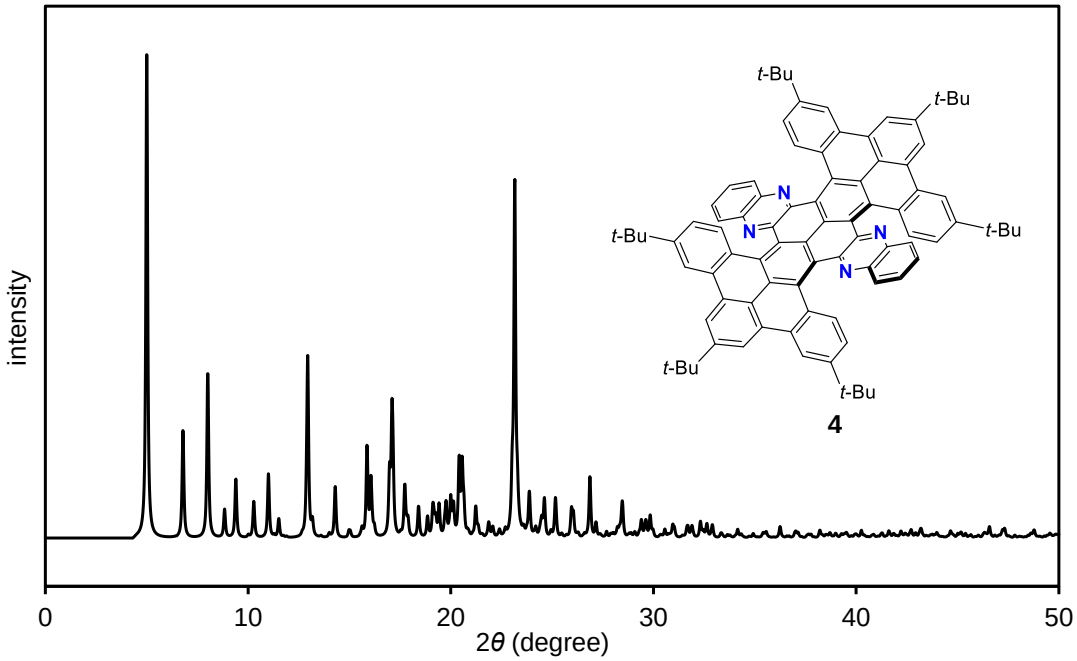

Figure S15. XRD spectrum of **4** from cif.

8. References

(1) Z. Xu, S. Meng, Z. Zhang, S. Han, F. Bai, Y. Dong, Y. Hashikawa, Chaolumen, *Precis. Chem.*, 2025. DOI: 10.1021/prechem.5c00001.

(2) G. M. Sheldrick, *Acta Crystallogr. Sect. A*, 2015, **71**, 3–8.